

# BofA protein inhibits intramembrane proteolysis of pro- $\sigma^K$ in an intercompartmental signaling pathway during *Bacillus subtilis* sporulation

Ruanbao Zhou and Lee Kroos\*

Department of Biochemistry and Molecular Biology, Michigan State University, East Lansing, MI 48824

Edited by Carol A. Gross, University of California, San Francisco, CA, and approved March 11, 2004 (received for review November 20, 2003)

*Bacillus subtilis* is a bacterium that undergoes a developmental program of sporulation in response to starvation. At the core of the program are  $\sigma$  factors, whose regulated spatiotemporal activation controls much of the gene expression. Activation of pro- $\sigma^K$  in the mother cell compartment involves regulated intramembrane proteolysis (RIP) in response to a signal from the forespore. RIP is a poorly understood process that is conserved in prokaryotes and eukaryotes. Here, we report a powerful system for studying RIP of pro- $\sigma^K$ . *Escherichia coli* was engineered to coexpress the putative membrane-embedded metalloprotease SpoIVFB with pro- $\sigma^K$  and potential inhibitors of RIP. Overproduction of SpoIVFB and pro- $\sigma^K$  in *E. coli* allowed accurate and abundant proteolytic processing of pro- $\sigma^K$  with the characteristics expected for SpoIVFB acting as an intramembrane-cleaving protease (I-Clip). Coexpression of BofA in this system led to formation of a BofA–SpoIVFB complex and marked inhibition of pro- $\sigma^K$  processing. Mutational analysis identified amino acids in BofA that are necessary for complex formation and inhibition of processing, leading us to propose that BofA inhibits SpoIVFB metalloprotease activity by providing a metal ligand, analogous to the cysteine switch mechanism of matrix metalloprotease regulation. The approach described herein should be applicable to studies of other RIP events and amenable to developing *in vitro* assays for I-Clips.

The abilities of cells to send signals, and to sense and respond to signals from other cells or from the environment, are essential features of developmental and adaptive processes. Regulated intramembrane proteolysis (RIP) has emerged as an important and widely conserved mechanism for controlling signaling pathways in both prokaryotes and eukaryotes (1). RIP involves cleavage of a protein in a transmembrane domain, releasing a part of the protein that in most cases regulates transcription or acts as a signal. Proteases believed to catalyze intramembrane cleavage occur in large families that are typically conserved from archaea to humans, and sometimes in bacteria as well (2). For example, one of the first intramembrane-cleaving proteases (I-Clips) identified, human site-2 protease (S2P) (3), has orthologs in *Bacillus subtilis* (SpoIVFB) (4, 5) and *Escherichia coli* (YaeL) (6, 7). Also, *Drosophila* and bacterial I-Clips in the rhomboid family recognize the same substrate motif and can be functionally interchanged (8, 9). RIP has been implicated in generating bacterial mating (10) and quorum sensing signals (11), and in the extracytoplasmic stress response of *E. coli* (6, 7). In metazoans, RIP is believed to control the unfolded protein stress response, cholesterol and fatty acid biosynthesis, epidermal growth factor and ErbB4 receptor signaling, Notch signaling, and processing of the Alzheimer precursor protein (1, 2). Elucidating mechanisms of RIP is important for understanding diverse signaling pathways and potentially for treating disease.

Bacterial sporulation provides a model to study RIP. When starved, certain bacteria undergo endospore formation, in which the cell is divided into mother cell and forespore compartments. Differential gene expression in the two compartments ensues, and signaling between the compartments ensures coordinate gene regulation and morphogenesis (12). One of the signaling

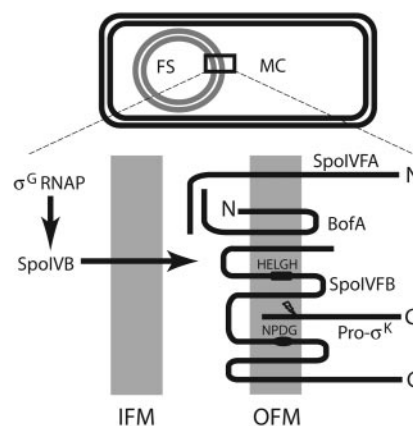


**Fig. 1.** Model showing proteins involved in the  $\sigma^K$  checkpoint. (Upper) A sporangium in which the forespore (FS) has been engulfed within the mother cell (MC). (Lower) An expanded view of the inner forespore membrane (IFM) and the outer forespore membrane (OFM), which surround the FS.  $\sigma^G$  RNA polymerase ( $\sigma^G$  RNAP) transcribes *spoIVB* in the FS (21). SpoIVB (not to be confused with SpoIVFB) is believed to cross the IFM and activate pro- $\sigma^K$  processing by SpoIVFB (lightning bolt). The topologies depicted for BofA, SpoIVFA, and SpoIVFB are based on analysis of *lacZ* and *phoA* fusions in *E. coli* (34, 40). The HELGH and NPDG sequences of SpoIVFB that are critical for RIP of pro- $\sigma^K$  (4, 5), are predicted to be in transmembrane segments. Release of  $\sigma^K$  from the OFM allows formation of  $\sigma^K$  RNA polymerase in the MC, which transcribes genes whose products help form the cortex and coat layers of the spore.

pathways in *B. subtilis*, termed the  $\sigma^K$  checkpoint (Fig. 1) (13), appears to involve RIP.  $\sigma^K$  is synthesized as an inactive precursor, pro- $\sigma^K$ , that associates with membranes in cells (13–15). SpoIVFB is believed to be an I-Clip that processes pro- $\sigma^K$  to  $\sigma^K$  on the basis of the following: a *B. subtilis spoIVFB* mutant is defective in processing (14), coexpression of *spoIVFB* and *sigK* (encoding pro- $\sigma^K$ ) in growing *B. subtilis* allows processing (16, 17), SpoIVFB is a membrane protein (18) with sequence similarity to the S2P family of I-Clips (4, 5, 19), and mutational analysis of conserved motifs in apparent transmembrane segments of SpoIVFB supports the idea that it is a metalloprotease (4, 5). However, as is the case for all I-Clips, cleavage of a physiological substrate *in vitro* with purified enzyme has not been accomplished.

Also lacking is an understanding of how pro- $\sigma^K$  processing is regulated. SpoIVFB forms a complex with SpoIVFA and BofA in the outer forespore membrane (OFM) (Fig. 1) (18, 20). This

This paper was submitted directly (Track II) to the PNAS office.

Abbreviations: RIP, regulated intramembrane proteolysis; I-Clip, intramembrane-cleaving protease; OFM, outer forespore membrane; IFM, inner forespore membrane; Km<sup>R</sup>, kanamycin-resistant; Ap<sup>R</sup>, ampicillin-resistant; IPTG, isopropyl  $\beta$ -D-thiogalactopyranoside.

\*To whom correspondence should be addressed. E-mail: kroos@msu.edu.

© 2004 by The National Academy of Sciences of the USA

**Table 1. Plasmids used in this study**

Plasmid	Description
pETpro- $\sigma^K$	Km <sup>R</sup> ; T7-pro- $\sigma^K$ H6*
pZR2	Ap <sup>R</sup> ; T7-H10SpoIVFB-GFP
pZR6	Km <sup>R</sup> ; T7-H10SpoIVFB-GFP
pZR12	Km <sup>R</sup> ; T7-pro- $\sigma^K$ (1–126)H6
pZR13	Ap <sup>R</sup> ; T7-H10SpoIVFB-GFP
pZR16	Ap <sup>R</sup> ; T7-H10SpoIVFB-GFP/T7-BofA
pZR24	Ap <sup>R</sup> ; T7-H10SpoIVFB-E44Q-GFP
pZR33	Ap <sup>R</sup> ; T7-H10SpoIVFB-GFP/SpoIVFA
pZR62	Ap <sup>R</sup> ; T7-GFP $\Delta$ 27BofA
pZR63	Km <sup>R</sup> ; T7-pro- $\sigma^K$ (1–126)H6/T7-GFP $\Delta$ 27BofA
pZR64	Ap <sup>R</sup> ; T7-GFP $\Delta$ 27BofA-G75E
pZR65	Ap <sup>R</sup> ; T7-GFP $\Delta$ 27BofA-H57F
pZR67	Ap <sup>R</sup> ; T7-H10SpoIVFB-GFP/T7-GFP $\Delta$ 27BofA
pZR68	Ap <sup>R</sup> ; T7-H10SpoIVFB-GFP/T7-GFP $\Delta$ 27BofA-G75E
pZR70	Km <sup>R</sup> ; T7-pro- $\sigma^K$ (1–126)H6/T7-GFP $\Delta$ 27BofA-H57F
pZR73	Ap <sup>R</sup> ; T7-SpoIVFA

Km<sup>R</sup>, kanamycin-resistant; Ap<sup>R</sup>, ampicillin-resistant.

\*The T7 RNA polymerase promoter (T7) plus the optimum translation initiation sequence in pET-29b was fused to the *B. subtilis* sigK gene (encoding pro- $\sigma^K$ ) which had been tagged with six histidine (H6) residues at the C-terminus (40). The descriptions of other plasmids are abbreviated in a similar fashion, and details of their construction are in Tables 2 and 3.

complex appears to be inactive for pro- $\sigma^K$  processing, and it is thought to be activated by SpoIVB, a serine protease synthesized in the forespore that is believed to traverse the inner forespore membrane (IFM) (21–23). The observation that BofA stabilizes SpoIVFA led to the model that SpoIVFA inhibits SpoIVFB I-Clip activity until the SpoIVB signal comes from the forespore (24). The level of SpoIVFA decreases when pro- $\sigma^K$  processing begins during sporulation, and the decrease of SpoIVFA depends on SpoIVB (25, 26). However, a form of SpoIVFA made more stable by fusion with the green fluorescent protein (GFP) did not prevent processing (20). Also, conditions were found under which the level of SpoIVFA decreased, but SpoIVFB did not become active for processing of pro- $\sigma^K$  (25). These results suggested that SpoIVFA might not be the primary inhibitor of SpoIVFB. Because SpoIVFA localizes to the membrane surrounding the forespore and helps BofA and SpoIVFB to do likewise, SpoIVFA was proposed to assemble a complex in which BofA inhibits SpoIVFB I-Clip activity (20).

Here, we show that SpoIVFB is sufficient for accurate and abundant proteolytic processing of pro- $\sigma^K$  in a heterologous host. By expressing different components of the  $\sigma^K$  checkpoint in *E. coli*, we demonstrate that BofA can inhibit pro- $\sigma^K$  processing in the absence of SpoIVFA. We present a model for the mechanism by which BofA inhibits SpoIVFB I-Clip activity, based on analogy with matrix metalloprotease inhibition and the results of mutations in *bofA*. We discuss RIP of pro- $\sigma^K$  in light of the recent finding that the SpoIVB serine protease can cleave SpoIVFA *in vitro* (26).

## Materials and Methods

**Plasmids.** The plasmids used in this study are described briefly in Table 1. Details of their construction are in Tables 2 and 3, which are published as supporting information on the PNAS web site. The methods used have been described previously (27). DNA sequencing of all cloned PCR products and all genes subjected to mutagenesis (QuikChange kit, Stratagene) confirmed the presence of the desired sequences.

**Cotransformation and Protein Production.** Proteins were produced in the *E. coli* strain BL21(DE3) (Novagen), which can be induced to synthesize T7 RNA polymerase. To transform this strain with

two plasmids bearing different antibiotic resistance genes and different *B. subtilis* genes fused to a T7 RNA polymerase promoter, 50 ng of each plasmid was electroporated into cells, and transformants were selected on Luria–Bertani (LB) agar supplemented with kanamycin sulfate (50  $\mu$ g/ml) and ampicillin (100  $\mu$ g/ml). To induce expression, transformants were grown in LB liquid containing 50  $\mu$ g/ml kanamycin and 200  $\mu$ g/ml ampicillin overnight at 37°C with shaking at 350 rpm, then 200  $\mu$ l of culture was transferred to 10 ml of fresh LB liquid with antibiotics, and incubation was continued under the same conditions until the culture reached an optical density at 600 nm (OD<sub>600</sub>) of 0.7–0.8, at which time isopropyl  $\beta$ -D-thiogalactopyranoside (IPTG) (0.5 mM) was added and incubation was continued for 2 h.

**Western Blot Analysis.** Equivalent amounts of *E. coli* cells from different cultures were collected from 0.5–1.0 ml of culture (depending on the OD<sub>600</sub>) by centrifugation (12,000  $\times$  g). Unless otherwise specified, extracts were prepared by resuspending cells in 50  $\mu$ l of lysis buffer [50 mM Tris-HCl, pH 7.5/10 mM MgCl<sub>2</sub>/1 mM EDTA/1 mM Pefabloc (Roche Molecular Biochemicals)/1 mg/ml lysozyme/10  $\mu$ g/ml DNase I] and incubating for 10 min at 37°C, then adding 50  $\mu$ l of 2 $\times$  sample buffer [50 mM Tris-HCl, pH 6.8/4% SDS/20% (vol/vol) glycerol/200 mM DTT/0.03% bromophenol blue] and boiling for 3 min. After centrifugation (12,000  $\times$  g), 2  $\mu$ l of supernatant was loaded onto an SDS/14% Prosieve polyacrylamide gel (Cambrex Bio Science, Rockland, ME) for separation of proteins and Western blot analysis as described previously (25). Antibodies to pentahistidine (Qiagen, Valencia, CA) were used at 1:10,000 dilution.

**Fractionation of Cellular Proteins.** *E. coli* from cultures (100 ml) induced as described above were harvested by centrifugation (12,000  $\times$  g) and resuspended in 6 ml of PBS, pH 7.2 (Invitrogen), containing 1 mM Pefabloc, 0.5 mg/ml lysozyme, 10  $\mu$ g/ml DNase I, and 10  $\mu$ g/ml RNase A, then passed twice through a French pressure cell (American Instruments) at 14,000 lb/in<sup>2</sup> (96 MPa). The lysate was centrifuged at 4°C (12,000  $\times$  g, 10 min). The supernatant (4.5 ml) was centrifuged at 4°C for 1.5 h at 200,000  $\times$  g in a SW50.1 rotor (Beckman). The supernatant served as the cytoplasmic fraction. The pellet was rinsed with PBS, then resuspended in PBS (4.5 ml), and this served as the membrane fraction. To 50  $\mu$ l of each fraction, 50  $\mu$ l of 2 $\times$  sample buffer was added. The samples were boiled for 3 min, then subjected to Western blot analysis.

## Membrane Solubilization and Affinity Purification of Complexes.

Membrane pellets prepared as described above were solubilized with 600  $\mu$ l of detergent buffer (PBS, pH 7.2/1% digitonin/150 mM NaCl/10% glycerol/1 mM Pefabloc) by rotating for 2 h at 4°C. Samples were then centrifuged at 4°C for 1 h at 100,000  $\times$  g in a SW50.1 rotor. The supernatant (500  $\mu$ l) was collected and diluted with 500  $\mu$ l of buffer (PBS, pH 7.2/150 mM NaCl, 1 mM Pefabloc). A sample (50  $\mu$ l) was taken to represent the input, then the rest was mixed with 100  $\mu$ l cobalt resin slurry (Clontech) by rotating for 1 h at 4°C. Resin was collected by centrifugation at 1,000  $\times$  g, washed three times with buffer (PBS, pH 7.2/150 mM NaCl/10 mM imidazole/5% glycerol/1 mM Pefabloc), then eluted with 60  $\mu$ l of buffer (1 $\times$  sample buffer containing 200 mM imidazole, 300 mM NaCl, and 10 mM EDTA) by incubating at 50°C for 20 min. A sample (10  $\mu$ l) was subjected to Western blot analysis.

## Results

**Accurate and Abundant Pro- $\sigma^K$  Processing in *E. coli*.** Coexpression of a C-terminally 6-histidine-tagged pro- $\sigma^K$  (denoted pro- $\sigma^K$ H6) with an N-terminally 10-histidine- and C-terminally GFP-tagged SpoIVFB (denoted H10SpoIVFB-GFP) in *E. coli* BL21(DE3)

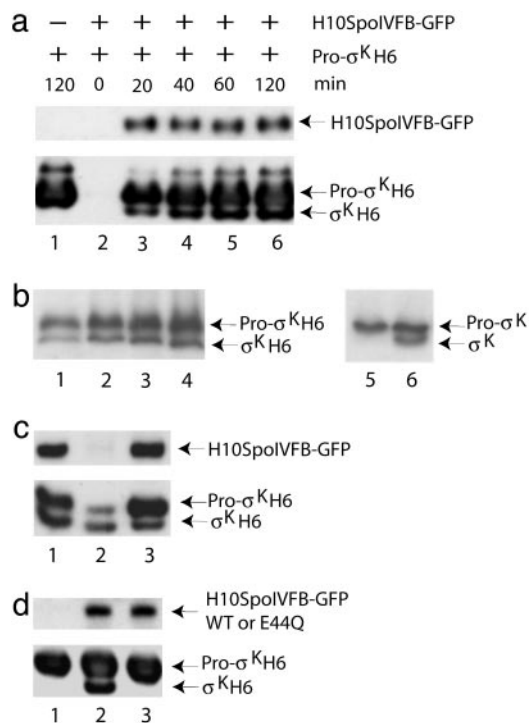


**Fig. 2.** Accurate and abundant pro- $\sigma^K$  processing in *E. coli*. (a) Western blot analysis of H10SpoIVFB-GFP and pro- $\sigma^K$ H6/ $\sigma^K$ H6 by using penta-His antibodies. Samples were collected at the indicated times after IPTG induction of *E. coli* bearing only pETpro- $\sigma^K$  (lane 1) or both pETpro- $\sigma^K$  and pZR2 (lanes 2–6). (b) Comparison of pro- $\sigma^K$  processing in *E. coli* and in sporulating *B. subtilis* PY79 (41). Whole-cell extracts were subjected to Western blot analysis with antibodies against pro- $\sigma^K$ . *E. coli* bearing pETpro- $\sigma^K$  and pZR2 was induced with IPTG for 1 h, extract was prepared and diluted 1,000-fold, then 2 (lane 1), 4 (lane 2), 6 (lane 3), or 8  $\mu$ l (lane 4) was analyzed. An equivalent amount of *B. subtilis* (based on the OD<sub>600</sub> of the culture) was analyzed at hour 3 (lane 5) and hour 4 (lane 6) of sporulation, using 6  $\mu$ l of undiluted extract. (c) Fractionation of cell extracts. *E. coli* bearing pETpro- $\sigma^K$  and pZR2 was induced with IPTG for 2 h. The whole-cell lysate after low-speed (12,000  $\times$  g) centrifugation (lane 1) and the cytoplasmic (lane 2) and membrane (lane 3) fractions were subjected to Western blot analysis with antibodies against GFP (Upper) or pro- $\sigma^K$  (Lower). (d) Effect of an E44Q change in H10SpoIVFB-GFP. *E. coli* bearing pETpro- $\sigma^K$  alone (lane 1) or in combination with pZR2 (lane 2) or pZR24 (lane 3) was induced with IPTG for 2 h, and extracts were subjected to Western blot analysis with penta-His antibodies.

resulted in processing of pro- $\sigma^K$ H6 (Fig. 2a, lanes 3–6). Processing depended absolutely on H10SpoIVFB-GFP (Fig. 2a, lane 1). The N-terminal amino acid sequence of the processed pro- $\sigma^K$ H6 (denoted  $\sigma^K$ H6) was determined by Edman degradation to be YVKNNAPF, which is identical to that of  $\sigma^K$  from sporulating *B. subtilis* (28), so processing was accurate.

Processing was also abundant in the heterologous host. The engineered *E. coli* synthesized at least 20 times more SpoIVFB (data not shown) and produced about 1,000 times more  $\sigma^K$  than an equivalent amount of sporulating *B. subtilis* (Fig. 2b, compare lanes 3 and 6). Fractionation of cell extracts showed that H10SpoIVFB-GFP is present only in the membrane fraction, as is the majority of pro- $\sigma^K$ H6 (Fig. 2c, lane 3). Taken together, our results demonstrate that SpoIVFB is sufficient for accurate and abundant processing of pro- $\sigma^K$  in *E. coli*.

In support of the model that SpoIVFB is a metalloprotease with a transmembrane <sup>43</sup>HEXXH<sup>47</sup> motif (Fig. 1) in which the conserved glutamic acid (E44) promotes nucleophilic attack by a water molecule on the carbonyl atom of the substrate peptide bond, changing E44 of H10SpoIVFB-GFP to glutamine abol-

ished processing of pro- $\sigma^K$ H6 in *E. coli* (Fig. 2d, lane 3), just as this mutation blocked processing in *B. subtilis* (4, 5).

**BofA Alone Can Inhibit Processing of Pro- $\sigma^K$ .** Both BofA and SpoIVFA are necessary to inhibit pro- $\sigma^K$  processing during *B. subtilis* sporulation, until a signal from the forespore overcomes the inhibition (13, 21, 29). Recently, two studies have suggested that BofA might be the primary inhibitor of SpoIVFB I-Clip activity, with SpoIVFA aiding in assembly and stabilization of an inhibited complex (20, 25). If this model is correct, we reasoned that overproduction of BofA in the *E. coli* system might alleviate the need for SpoIVFA and enable BofA alone to inhibit SpoIVFB.

*E. coli* engineered to overproduce BofA, in addition to H10SpoIVFB-GFP and pro- $\sigma^K$ H6, showed a substantial reduction in the level of  $\sigma^K$ H6 (Fig. 3a, lane 3), consistent with the notion that BofA can inhibit SpoIVFB I-Clip activity. In contrast, production of SpoIVFA had little or no effect on the  $\sigma^K$ H6 level (Fig. 3a, lane 4).

Amino acids 1 through 126 of pro- $\sigma^K$ , denoted pro- $\sigma^K$ (1–126), are sufficient to serve as a substrate for RIP in sporulating *B. subtilis* (H. Prince and L.K., unpublished data). This truncated form of pro- $\sigma^K$  is also processed in *E. coli*, if H10SpoIVFB-GFP is coexpressed (Fig. 3b, lane 2). The N-terminal amino acid sequence of the product after processing was determined by Edman degradation to be identical to that of  $\sigma^K$ H6 produced in *E. coli* and that of  $\sigma^K$  produced in sporulating *B. subtilis* (28), indicating that processing of pro- $\sigma^K$ (1–126)H6 is accurate and produces a product we denote  $\sigma^K$ (21–126)H6. Processing appeared to be inhibited by BofA (Fig. 3b, lane 4), but not by SpoIVFA (Fig. 3b, lane 3). Because it was easier to separate pro- $\sigma^K$ (1–126)H6 from  $\sigma^K$ (21–126)H6 by SDS/PAGE than for the full-length proteins, the C-terminally truncated pro- $\sigma^K$  was used in subsequent experiments.

The reduction in the level of  $\sigma^K$ (21–126)H6 in *E. coli* engineered to overproduce BofA (Fig. 3b, lane 4) did not result from a change in the stability of  $\sigma^K$ (21–126)H6. These cells exhibited kinetics of  $\sigma^K$ (21–126)H6 loss after inhibition of translation by chloramphenicol (200 mg/ml) similar to those of cells not producing BofA (data not shown). Also, BofA did not impair accumulation of pro- $\sigma^K$ (1–126)H6 (Fig. 3b, lane 4). Hence, BofA did not appear to have an indirect effect on substrate availability or product stability.

GFP $\Delta$ 27BofA is a fusion of GFP to amino acid 28 of BofA, which was shown previously to be fully functional in *B. subtilis* and allow detection of the protein by Western blotting with anti-GFP antibodies (20). When overproduced in *E. coli*, GFP $\Delta$ 27BofA was present exclusively in the membrane fraction (Fig. 3c, lane 1), and it appeared to inhibit pro- $\sigma^K$ (1–126)H6 processing (Fig. 4a, lane 2) to an extent similar to that of BofA (Fig. 3b, lane 4). SpoIVFA was also present only in the membrane fraction (Fig. 3c, lane 3), so its lack of an effect on processing (Fig. 3b, lane 3) did not appear to result from mislocalization.

To test whether BofA or SpoIVFA forms a complex with SpoIVFB in *E. coli*, we made use of the observation that a BofA–SpoIVFA–SpoIVFB complex can be solubilized from membranes of sporulating *B. subtilis* with the nonionic detergent digitonin (20). Membranes from *E. coli* overproducing GFP $\Delta$ 27BofA or SpoIVFA, and H10SpoIVFB-GFP, were solubilized, then complexes were affinity-purified with cobalt resin, to which the 10-His tag on H10SpoIVFB-GFP was expected to bind. GFP $\Delta$ 27BofA copurified with H10SpoIVFB-GFP (Fig. 3d, lane 2) and did not bind to the cobalt resin in the absence of H10SpoIVFB-GFP (Fig. 3d, lane 1). SpoIVFA did not copurify with H10SpoIVFB-GFP (Fig. 3d, lane 4). These results demonstrate that GFP $\Delta$ 27BofA forms a complex with H10SpoIVFB-GFP in *E. coli*, supporting the idea that BofA directly inhibits

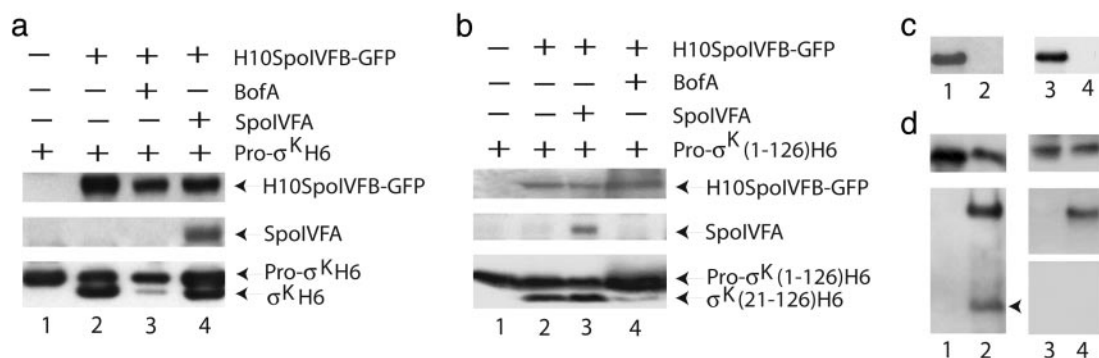


**Fig. 3.** BofA inhibits processing of pro- $\sigma^K$ . (a) Effects of BofA or SpoIVFA on processing of pro- $\sigma^K$ H6. *E. coli* cells bearing pETpro- $\sigma^K$  alone (lane 1) or in combination with pZR2 (lane 2), pZR16 (lane 3), or pZR33 (lane 4), were induced with IPTG for 2 h to express the indicated proteins. Extracts were prepared as described for fractionation of cellular proteins (*Materials and Methods*) and the whole-cell lysates after low-speed ( $12,000 \times g$ ) centrifugation were subjected to Western blot analysis using antibodies against GFP (*Top*), SpoIVFA (*Middle*), or penta-His (*Bottom*). (b) Effect of BofA or SpoIVFA on processing of pro- $\sigma^K$ (1-126)H6. *E. coli* cells bearing pZR12 alone (lane 1) or in combination with pZR13 (lane 2), pZR33 (lane 3), or pZR16 (lane 4) were induced with IPTG for 2 h, then whole-cell extracts were subjected to Western blot analysis using antibodies against penta-His (*Top and Bottom*) or SpoIVFA (*Middle*). (c) Membrane association of GFP $\Delta$ 27BofA and SpoIVFA. Membrane (lanes 1 and 3) and cytoplasmic (lanes 2 and 4) fractions of *E. coli* bearing pZR63 (lanes 1 and 2) or pZR33 (lanes 3 and 4), which had been induced with IPTG for 2 h, were subjected to Western blot analysis with antibodies against GFP (lanes 1 and 2, to detect GFP $\Delta$ 27BofA) or SpoIVFA (lanes 3 and 4). (d) Membrane solubilization and affinity purification of complexes. Detergent-solubilized membranes from *E. coli* bearing pZR62 alone (lane 1) or in combination with pZR6 (lane 2), or bearing pZR73 alone (lane 3) or in combination with pZR6 (lane 4), were subjected to Western blot analysis before (*Upper*) or after (*Lower*) affinity purification of complexes (*Materials and Methods*), using antibodies against GFP (lanes 1 and 2, *Upper* shows GFP $\Delta$ 27BofA, *Lower* shows H10SpoIVFB-GFP as the upper band and GFP $\Delta$ 27BofA marked with an arrowhead) or, for lanes 3 and 4, antibodies against SpoIVFA (*Top and Bottom*) or against GFP (*Middle*, to detect H10SpoIVFB-GFP).

SpoIVFB I-Clip activity to bring about the observed reduction in the level of  $\sigma^K$ (21-126)H6 (Fig. 3b, lane 4).

**Specificity of Inhibition by BofA.** It was conceivable that formation of an inhibitory complex with SpoIVFB was an artifact of BofA overproduction in *E. coli*. To test the specificity of the inhibition, we made a single amino acid change in BofA. Previous studies showed that changing the glycine at position 75 to glutamic acid (denoted G75E) impaired BofA's ability to inhibit pro- $\sigma^K$  processing in sporulating *B. subtilis* (13, 30). We engineered this change into the gene encoding GFP $\Delta$ 27BofA so we could detect the mutant protein.

The G75E change in GFP $\Delta$ 27BofA impaired its ability to inhibit processing (Fig. 4a, lane 3), despite accumulation of the mutant protein to a level similar to that of wild-type GFP $\Delta$ 27BofA (Fig. 4a *Middle*). Unlike the wild-type protein, a substantial amount of GFP $\Delta$ 27BofA G75E was present in the cytoplasmic fraction (Fig. 4c, lane 2), although a slight majority was in the membrane fraction (Fig. 4c, lane 1). However, GFP $\Delta$ 27BofA G75E failed to copurify with H10SpoIVFB-GFP after membrane solubilization (Fig. 4d, lane 2). It appears that the G75E change impairs BofA's ability to interact with the SpoIVFB metalloprotease and inhibit intramembrane proteolysis of pro- $\sigma^K$ .

**Mechanism of Inhibition by BofA.** We considered the possibility that BofA inhibits SpoIVFB by a mechanism analogous to the cysteine switch observed for matrix metalloproteases (31-33). These enzymes are synthesized as latent proenzymes in which the sulfhydryl group of a cysteine residue in the propeptide coordinates the catalytic zinc ion. Interruption of this interaction activates the metalloprotease. By analogy, BofA could provide a ligand to the putative metal ion of SpoIVFB, blocking the active site. GFP $\Delta$ 27BofA has two potential metal ligands. Alignment of BofA orthologs from *B. subtilis*, *Bacillus halodurans*, *Bacillus cereus*, and *Bacillus anthracis* revealed that histidine-57, but not cysteine-46, is conserved (Fig. 6, which is published as supporting information on the PNAS web site). Changing the histidine at position 57 to phenylalanine (denoted H57F) in GFP $\Delta$ 27BofA markedly impaired the ability of the protein to

inhibit processing of pro- $\sigma^K$ (1-126)H6 in *E. coli* (Fig. 4b, lane 3). The H57F mutant protein accumulated to a level similar to that of the wild-type protein (Fig. 4b, *Middle*), and GFP $\Delta$ 27BofA H57F was almost exclusively membrane-associated (Fig. 4c), but it failed to copurify with H10SpoIVFB-GFP after membrane solubilization (Fig. 4d, lane 4). GFP $\Delta$ 27BofA H57F also was impaired in its ability to inhibit pro- $\sigma^K$  processing in sporulating *B. subtilis*, despite accumulating to a level similar to that of the wild-type protein (Fig. 7, which is published as supporting information on the PNAS web site). In contrast to the H57F substitution in BofA, a C46S change had no effect on its ability to inhibit processing in *E. coli* (data not shown). These results support a model in which H57 of BofA is a ligand of zinc in SpoIVFB and thereby prevents intramembrane proteolysis of pro- $\sigma^K$ .

## Discussion

We have established a powerful system for studying RIP of pro- $\sigma^K$  and used it to provide evidence that BofA is the primary inhibitor of SpoIVFB I-Clip activity. Our results suggest that a similar approach of overproducing I-Clips, their substrates, and potential regulatory proteins in *E. coli*, or another vector/host system such as baculovirus-infected insect cells, could be applied to investigate other RIP events.

The large amount of  $\sigma^K$  produced in *E. coli* engineered to overproduce H10SpoIVFB-GFP suggests that these cells are the best available starting material for attempts aimed at purifying SpoIVFB and demonstrating I-Clip activity *in vitro*. The engineered *E. coli* produced about 1,000-fold more  $\sigma^K$  (Fig. 2b) and at least 20-fold more H10SpoIVFB-GFP (data not shown) than sporulating *B. subtilis* expressing *sigK* (encoding pro- $\sigma^K$ ) and *spoIVFB-gfp* from native promoters. Overproducing pro- $\sigma^K$  in sporulating *B. subtilis* did not increase the  $\sigma^K$  level, as if the protease was limiting (14). Also, expressing *sigK* and *spoIVFB-gfp* from a xylose-inducible promoter in growing *B. subtilis* did not result in more  $\sigma^K$  produced per cell (17).

Despite the 1,000-fold increase in the  $\sigma^K$  level in our engineered *E. coli*, there appears to be room for improvement. Much pro- $\sigma^K$  remains unprocessed in the whole-cell extract 2 h after induction with IPTG (Fig. 2a). However, more than half of the

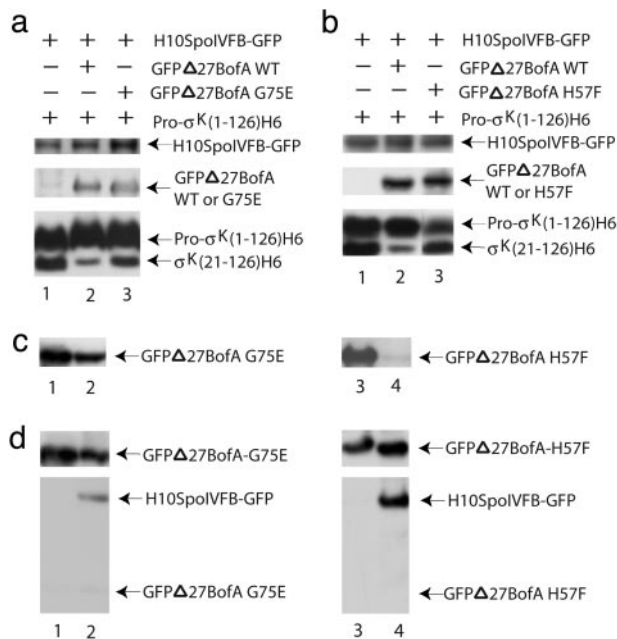


**Fig. 4.** Amino acid substitutions in BofA impair its ability to inhibit pro- $\sigma^K(1-126)H6$  processing. (a) Effect of a G75E change in BofA. *E. coli* cells bearing pZR12 and pZR13 (lane 1), pZR67 (lane 2), or pZR68 (lane 3) were induced with IPTG for 2 h to express the indicated proteins. Whole-cell extracts were subjected to Western blot analysis using antibodies against GFP (Top and Middle) or penta-His (Bottom). (b) Effect of a H57F change in BofA. *E. coli* strains were the same as in a, except lane 3 contained an extract from *E. coli* bearing pZR13 and pZR70. (c) Membrane association of mutant BofA proteins. Membrane (lanes 1 and 3) and cytoplasmic (lanes 2 and 4) fractions of *E. coli* bearing pZR64 (lanes 1 and 2) or pZR65 (lanes 3 and 4), which had been induced with IPTG for 2 h, were subjected to Western blot analysis with antibodies against GFP. (d) Membrane solubilization and affinity purification of complexes. Detergent-solubilized membranes from *E. coli* bearing pZR64 alone (lane 1) or in combination with pZR6 (lane 2), or bearing pZR65 alone (lane 3) or in combination with pZR6 (lane 4), were subjected to Western blot analysis before (Upper) or after (Lower) affinity purification of complexes, using antibodies against GFP.

overproduced pro- $\sigma^K$  is probably inaccessible for RIP, because it pellets upon low-speed centrifugation, suggesting it forms insoluble aggregates (compare the whole-cell extract shown in Fig. 2a, lane 6, with the supernatant after low-speed centrifugation shown in Fig. 2c, lane 1). Nevertheless, a substantial amount of pro- $\sigma^K$  is membrane-associated, but not processed (Fig. 2c, lane 3), so SpoIVFB I-Clip activity may be limiting. Alternatively, a factor that stimulates pro- $\sigma^K$  processing in sporulating *B. subtilis* may be missing or suboptimal in the heterologous *E. coli* host.

By overproducing BofA in our *E. coli* system, we discovered that BofA is sufficient to markedly inhibit pro- $\sigma^K$  processing, providing experimental evidence that BofA is the primary inhibitor of SpoIVFB I-Clip activity. In sporulating *B. subtilis*, both BofA and SpoIVFA are required to prevent processing of pro- $\sigma^K$  until the SpoIVB signal comes from the forespore (13, 21, 29). In the absence of SpoIVFA, GFP $\Delta$ 27BofA and SpoIVFB-GFP fail to localize to the OFM, and GFP $\Delta$ 27BofA and native SpoIVFB are less stable (20). In *E. coli*, GFP $\Delta$ 27BofA (Fig. 3c) and H10SpoIVFB-GFP (Fig. 2c) are stable and membrane-associated in the absence of SpoIVFA, and RIP of pro- $\sigma^K$  is inhibited (Fig. 3a and b). The inhibition appears to result from a direct interaction between GFP $\Delta$ 27BofA and H10SpoIVFB-GFP (Fig. 3d).

Our results with mutant BofA proteins provide insight into its possible mechanism of SpoIVFB inhibition. Previous mutational

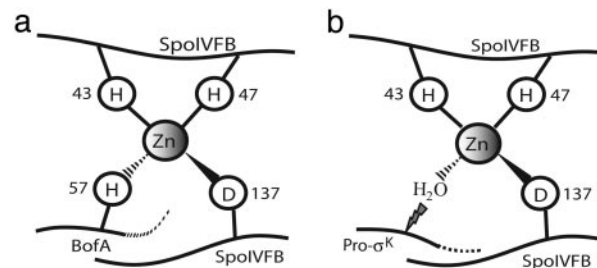


**Fig. 5.** Model for RIP of pro- $\sigma^K$ . (a) SpoIVFB is held inactive when H57 of BofA provides a fourth zinc ligand, in addition to H43, H47, and D137 of SpoIVFB (4, 5). This ligand provision is proposed to occur in the OFM in a complex that also includes SpoIVFA (not shown, see Fig. 1). (b) Loss of BofA, possibly brought about by cleavage of SpoIVFA by SpoIVB (26), allows zinc to activate a water molecule that hydrolyzes pro- $\sigma^K$ , releasing  $\sigma^K$  from the OFM into the mother cell cytoplasm, where it directs transcription of many genes.

analyses of *bofA* demonstrated that the C terminus plays a critical role in BofA function or stability (30, 34). Our analysis of GFP $\Delta$ 27BofA G75E in *E. coli* showed that the mutant protein accumulates as well as the wild-type protein (Fig. 4a), but the mutant protein was impaired in its ability to inhibit pro- $\sigma^K(1-126)H6$  processing (Fig. 4a) and was not found in complex with H10SpoIVFB-GFP (Fig. 4d). The correlation between loss of complex formation and loss of processing inhibition supports the idea that BofA must interact directly with SpoIVFB to inhibit its I-Clip activity. G75 is in a hydrophobic segment of BofA (amino acids 62–82) thought to be in the space between the IFM and OFM (Fig. 1) or possibly looping into the IFM (34). The latter hypothesis is supported by the existence of a proline residue at position 74, which may introduce a bend in the putative  $\alpha$ -helix. Perhaps the negative charge introduced by the G75E change perturbs the membrane topology of BofA so that it fails to interact properly with SpoIVFB.

Also in support of the idea that BofA directly inhibits SpoIVFB, GFP $\Delta$ 27BofA H57F was not found in complex with H10SpoIVFB-GFP (Fig. 4d) and was impaired in its ability to inhibit pro- $\sigma^K$  processing (Fig. 4b). We propose that H57 coordinates zinc in the active site of SpoIVFB (Fig. 5a), preventing access of a water molecule and the pro sequence of pro- $\sigma^K$ , which are necessary for peptide bond hydrolysis to produce  $\sigma^K$  (Fig. 5b). In this model, BofA function is analogous to that of the propeptide of matrix metalloproteases (31–33). A potential advantage of encoding the inhibitory peptide in a separate gene, as in the case of *bofA*, rather than in the same polypeptide, as for matrix metalloproteases, is the opportunity for separate transcriptional regulation of the protease and its inhibitor. Expression of *bofA* is strongly repressed by the mother cell transcription factor SpoIIID (35, 36), whereas expression of the *spoIVF* operon (encoding SpoIVFA and SpoIVFB) may be weakly inhibited by SpoIIID (29), but the significance of this regulation for the  $\sigma^K$  checkpoint has not yet been tested.

In orthologs of *B. subtilis* BofA found in closely related *Bacillus* species, H57 is conserved (Fig. 6), suggesting it also plays a crucial role in RIP of pro- $\sigma^K$  in these spore-forming bacteria, some of which are human pathogens. The genus *Clostridium* also includes pathogenic spore-formers, but the mechanisms of regulating  $\sigma^K$  activation appear to be different. In contrast to the situation in *B. subtilis*, where BofA and SpoIVFA work together to inhibit pro- $\sigma^K$  processing (13, 17, 20, 29, 30, 35), SpoIVFA orthologs are not found in the sequenced *Clostridium* genomes. Yet their SigK orthologs appear to have pro sequences, and putative metalloproteases with both the HEXXH and NPDG motifs can be found, although the latter exhibit low sequence similarity to SpoIVFB. Potential BofA orthologs are found in *Clostridium perfringens*, *Clostridium thermocellum*, and *Clostrid-*

*ium acetobutylicum*, albeit with less sequence similarity to *B. subtilis* BofA than for closely related *Bacillus* species. If the clostridia proteins are BofA homologs that inhibit SpoIVFB homologs, they must do so by a different mechanism than we have proposed for *B. subtilis* BofA (Fig. 5a), because H57 is not conserved in the clostridia proteins. Regulation of  $\sigma^K$  production has been shown to be achieved differently in *Clostridium difficile* (37). Its SigK ortholog has no pro sequence. A DNA rearrangement that excises a prophage-like insertion element in the *sigK* gene is a necessary step for efficient sporulation. The *B. subtilis* *sigK* gene normally undergoes a similar rearrangement (38), but substitution of an insertionless *sigK* gene for the normal gene does not impair sporulation (39), because RIP of pro- $\sigma^K$  still governs the production of active  $\sigma^K$ .

How is the SpoIVFA-BofA-SpoIVFB complex activated by the SpoIVB signal from the forespore during *B. subtilis* sporulation (Fig. 1)? Recently, Dong and Cutting (26) showed that the SpoIVB serine peptidase can cleave SpoIVFA when the two proteins are produced *in vitro*. These authors speculated that cleavage of SpoIVFA would dissolve the SpoIVFA-BofA-SpoIVFB complex, permitting SpoIVFB to cleave pro- $\sigma^K$ . However, our results show that BofA alone can interact with SpoIVFB and markedly inhibit RIP of pro- $\sigma^K$  (Fig. 3), raising the possibility that BofA might persist in complex with SpoIVFB, inhibiting its I-Clip activity, after cleavage of SpoIVFA. This possibility could explain the previous finding that translational arrest in sporulating *B. subtilis* leads to a decrease in the level of full-length SpoIVFA, but processing of pro- $\sigma^K$  is not observed (25). Perhaps when translation is blocked, mother cell proteases target SpoIVFA's N-terminal domain (Fig. 1), which may not be

necessary to maintain BofA inhibition of SpoIVFB I-Clip activity. During sporulation, SpoIVB might specifically target the C-terminal domain of SpoIVFA (26), which is believed to be located in the space between the IFM and OFM (Fig. 1), where it may interact with the C-terminal domain of BofA (30, 34, 40), facilitating its inhibition of SpoIVFB.

Although questions remain about RIP of pro- $\sigma^K$ , we have provided evidence that BofA is the primary inhibitor of SpoIVFB I-Clip activity. Other well studied I-Clips in the same family as SpoIVFB include human S2P (3) and *E. coli* YaeL (6, 7). These I-Clips do not appear to be regulated by an inhibitory protein. Rather, they operate in protease cascades in which their substrates must first be cleaved by a serine protease (1, 6, 7). There is no evidence to suggest that pro- $\sigma^K$  is cleaved before cleavage by SpoIVFB. However, it is interesting that SpoIVFB may still operate within a protease cascade, with a serine protease, SpoIVB, cleaving SpoIVFA and releasing BofA-mediated inhibition of SpoIVFB I-Clip activity, if the model of Dong and Cutting (26) is correct. More examples of RIP by I-Clips in this family will need to be studied to see whether prior substrate cleavage or prior cleavage of an inhibitory complex by a serine protease, or another mechanism, is the most common regulatory strategy.

We thank O. Resnekov, D. Rudner, and R. Losick for providing plasmids pOR267 and pdr95 and strains BDR511 and BDR88; S. Cutting for providing plasmid pET pro- $\sigma^K$  and strain SC599; H. Prince for providing plasmid pHP6; L. Gu for art work on the figures; and R. Britton and L. Snyder for critical reading of the manuscript. This research was supported by National Institutes of Health Grant GM43585 (to L.K.) and by the Michigan Agricultural Experiment Station.

- Brown, M. S., Ye, J., Rawson, R. B. & Goldstein, J. L. (2000) *Cell* **100**, 391–398.
- Urban, S. & Freeman, M. (2002) *Curr. Opin. Genet. Dev.* **12**, 512–518.
- Rawson, R., Zelenski, N., Nijhawan, D., Ye, J., Sakai, J., Hasan, M., Chang, T., Brown, M. & Goldstein, J. (1997) *Mol. Cell* **1**, 47–57.
- Rudner, D., Fawcett, P. & Losick, R. (1999) *Proc. Natl. Acad. Sci. USA* **96**, 14765–14770.
- Yu, Y.-T. N. & Kroos, L. (2000) *J. Bacteriol.* **182**, 3305–3309.
- Alba, B. M., Leeds, J. A., Onufryk, C., Lu, C. Z. & Gross, C. A. (2002) *Genes Dev.* **16**, 2156–2168.
- Kanehara, K., Ito, K. & Akiyama, Y. (2002) *Genes Dev.* **16**, 2147–2155.
- Urban, S., Schlieper, D. & Freeman, M. (2002) *Curr. Biol.* **12**, 1507–1512.
- Gallio, M., Sturgill, G., Rather, P. & Kysten, P. (2002) *Proc. Natl. Acad. Sci. USA* **99**, 12208–12213.
- An, F. Y., Sulavik, M. C. & Clewell, D. B. (1999) *J. Bacteriol.* **181**, 5915–5921.
- Rather, P. N., Ding, X., Baca-DeLancey, R. R. & Siddiqui, S. (1999) *J. Bacteriol.* **181**, 7185–7191.
- Stragier, P. & Losick, R. (1996) *Annu. Rev. Genet.* **30**, 297–341.
- Cutting, S., Oke, V., Driks, A., Losick, R., Lu, S. & Kroos, L. (1990) *Cell* **62**, 239–250.
- Lu, S., Halberg, R. & Kroos, L. (1990) *Proc. Natl. Acad. Sci. USA* **87**, 9722–9726.
- Zhang, B., Hofmeister, A. & Kroos, L. (1998) *J. Bacteriol.* **180**, 2434–2441.
- Lu, S., Cutting, S. & Kroos, L. (1995) *J. Bacteriol.* **177**, 1082–1085.
- Resnekov, O. & Losick, R. (1998) *Proc. Natl. Acad. Sci. USA* **95**, 3162–3167.
- Resnekov, O., Alper, S. & Losick, R. (1996) *Genes Cells* **1**, 529–542.
- Lewis, A. & Thomas, P. (1999) *Protein Sci.* **8**, 439–442.
- Rudner, D. Z. & Losick, R. (2002) *Genes Dev.* **16**, 1007–1018.
- Cutting, S., Driks, A., Schmidt, R., Kunkel, B. & Losick, R. (1991) *Genes Dev.* **5**, 456–466.
- Wakeley, P. R., Dorazi, R., Hoa, N. T., Bowyer, J. R. & Cutting, S. M. (2000) *Mol. Microbiol.* **36**, 1336–1348.
- Hoa, N. T., Brannigan, J. A. & Cutting, S. M. (2002) *J. Bacteriol.* **184**, 191–199.
- Resnekov, O. (1999) *J. Bacteriol.* **181**, 5384–5388.
- Kroos, L., Yu, Y. T., Mills, D. & Ferguson-Miller, S. (2002) *J. Bacteriol.* **184**, 5393–5401.
- Dong, T. C. & Cutting, S. M. (2003) *Mol. Microbiol.* **49**, 1425–1434.
- Sambrook, J., Fritsch, E. F. & Maniatis, T. (1989) *Molecular Cloning: A Laboratory Manual* (Cold Spring Harbor Lab. Press, Plainview, NY), 2nd Ed.
- Kroos, L., Kunkel, B. & Losick, R. (1989) *Science* **243**, 526–529.
- Cutting, S., Roels, S. & Losick, R. (1991) *J. Mol. Biol.* **221**, 1237–1256.
- Ricca, E., Cutting, S. & Losick, R. (1992) *J. Bacteriol.* **174**, 3177–3184.
- Springman, E., Angleton, E., Birkedal-Hansen, H. & Van Wart, H. (1990) *Proc. Natl. Acad. Sci. USA* **87**, 364–368.
- Van Wart, H. E. & Birkedal-Hansen, H. (1990) *Proc. Natl. Acad. Sci. USA* **87**, 5578–5582.
- Morgunova, E., Tuuttila, A., Bergmann, U., Isupov, M., Lindqvist, Y., Schneider, G. & Tryggvason, K. (1999) *Science* **284**, 1667–1670.
- Varcamonti, M., Marasco, R., De Felice, M. & Sacco, M. (1997) *Microbiology* **143**, 1053–1058.
- Ireton, K. & Grossman, A. (1992) *J. Bacteriol.* **174**, 3185–3195.
- Halberg, R. & Kroos, L. (1994) *J. Mol. Biol.* **243**, 425–436.
- Haraldsen, J. D. & Sonenshein, A. L. (2003) *Mol. Microbiol.* **48**, 811–821.
- Stragier, P., Kunkel, B., Kroos, L. & Losick, R. (1989) *Science* **243**, 507–512.
- Kunkel, B., Losick, R. & Stragier, P. (1990) *Genes Dev.* **4**, 525–535.
- Green, D. & Cutting, S. (2000) *J. Bacteriol.* **182**, 278–285.
- Youngman, P., Perkins, J. B. & Losick, R. (1984) *Plasmid* **12**, 1–9.